Journal of Physiology (2002), **545.3**, *pp.* 945–960
DOI: 10.1113/jphysiol.2002.023390

www.jphysiol.org

Journal of Physiology

Active and passive membrane properties of rat sympathetic preganglionic neurones innervating the adrenal medulla

Jennifer M. M. Wilson, Elaine Coderre, Leo P. Renaud and David Spanswick *

*Neurosciences, Ottawa Health Research Institute, University of Ottawa, Ontario, Canada K1Y 4E9 and * Department of Biological Sciences, University of Warwick, Coventry CV4 7AL, UK*

The intravascular release of adrenal catecholamines is a fundamental homeostatic process mediated via thoracolumbar spinal sympathetic preganglionic neurones (AD-SPN). To understand mechanisms regulating their excitability, whole-cell patch-clamp recordings were obtained from 54 retrogradely labelled neonatal rat AD-SPN. Passive membrane properties included a mean resting membrane potential, input resistance and time constant of −62 ± 6 mV, 410 ± 241 MΩ and 104 ± 53 ms, respectively. AD-SPN were homogeneous with respect to their active membrane properties. These active conductances included transient outward rectification, observed as a delayed return to rest at the offset of the membrane response to hyperpolarising current pulses, with two components: a fast 4-AP-sensitive component (A-type conductance), contributing to the after-hyperpolarisation (AHP) and spike repolarisation; a slower prolonged Ba^{2+}-sensitive component (D-like conductance). All AD-SPN expressed a Ba^{2+}-sensitive instantaneous inwardly rectifying conductance activated at membrane potentials more negative than around −80 mV. A potassium-mediated, voltage-dependent sustained outward rectification activated at membrane potentials between −35 and −15 mV featured an atypical pharmacology with a component blocked by quinine, reduced by low extracellular pH and arachidonic acid, but lacking sensitivity to Ba^{2+}, TEA and intracellular Cs^{+}. This quinine-sensitive outward rectification contributes to spike repolarisation. Following block of potassium conductances by Cs^{+} loading, AD-SPN revealed the capability for autorhythmicity and burst firing, mediated by a T-type Ca^{2+} conductance. These data suggest the output capability is dynamic and diverse, and that the range of intrinsic membrane conductances expressed endow AD-SPN with the ability to generate differential and complex patterns of activity. The diversity of intrinsic membrane properties expressed by AD-SPN may be key determinants of neurotransmitter release from SPN innervating the adrenal medulla. However, factors other than active membrane conductances of AD-SPN must ultimately regulate the differential ratio of noradrenaline (NA) *versus* adrenaline (A) release secreted in response to various physiological and environmental demands.

(Received 9 May 2002; accepted after revision 24 September 2002; first published online 1 November 2002)
Corresponding author D. Spanswick: Department of Biological Sciences, University of Warwick, Coventry CV4 7AL, UK. Email: dspanswick@bio.warwick.ac.uk

Mass activation of the sympathoadrenal nervous system occurs in the reflex 'fight or flight' response, which is characterised by extensive release of adrenaline (A) and noradrenaline (NA) from the adrenal medulla into the bloodstream. This phenomenon is fundamental to the behavioural response to a threatening situation and leads to a redistribution of the blood supply and mobilisation of energy resources to those structures to be engaged in the behaviour. On a moment-to-moment basis, physiological stimuli like exposure to cold evoke a predominantly NA release, while hypoglycaemia primarily causes an increase in adrenaline release (e.g. see Gagner *et al.* 1985; Vollmer, 1996). These physiological responses suggest a functionally and anatomically distinct organisation of the autonomic pathways controlling adrenaline and NA release. The ratio of A:NA release under resting conditions is around 3:1 and the mechanisms by which this balance is regulated can reside at any level of the neuroaxis: peripherally, at the level of chromaffin cells (e.g. see Marley & Livett, 1987) and centrally where many areas, including the hypothalamus, thalamus, preoptic area, brainstem, forebrain bundle and ventromedial nucleus (e.g. see Matsui, 1979, 1987; Robinson *et al.* 1983), have been reported to be involved in the regulation of these hormones.

Within the central pathways, key components of the circuits modulating adrenal medulla function are the sympathetic preganglionic neurones (SPN). Sympathetic preganglionic neurone innervation of chromaffin cells is predominantly by way of the anterior greater splanchnic

nerve, with variation of stimulus frequency of these axons being an important determinant of catecholamine release (Bloom *et al.* 1988; Edwards & Jones, 1993). Chromaffin cells receive axons directly from SPN located between thoracic segments 4–12 with the densest projection between T7–9 (Strack *et al.* 1989). Sympathetic preganglionic neurones whose axons project to the adrenal medulla (AD-SPN) have been shown to be sub-divisible in cat with respect to the calcium binding protein, calretinin (Edwards *et al.* 1996). In rat NA and adrenaline chromaffin cell-innervating SPN can be identified by their differential responses to electrical stimulation of the rostral ventro-lateral medulla (RVLM), reflex response to glucopenic stimuli and chemoreceptor and baroreceptor reflexes (Cao & Morrison 2000, 2001; Morrison & Cao 2000). These data further suggest functionally and anatomically separate central pathways for adrenaline and NA release. However, little known are the intrinsic mechanisms and membrane receptor profiles responsible for formulating the final central drive to the adrenal medulla, or whether differential expression of intrinsic membrane properties of AD-SPN contributes to the differential release of NA and adrenaline release. Data presented in the present study describe for the first time intrinsic membrane properties of AD-SPN. The largely homogeneous distribution of intrinsic active conductances across the AD-SPN population suggests that additional factors contribute to the differential regulation of adrenaline *versus* NA secretion.

METHODS

All experiments were performed in accordance with the guidelines of the Animal Care Committee of the Ottawa Health Research Institute.

Pre-labelling of SPN

Sympathetic preganglionic neurones were pre-labelled using methods similar to those previously reported (Spanswick *et al.* 1998). Briefly, neonatal rats (7–12 days) were deeply anaesthetised with halothane (4 % in O_2). Pedal and tail reflexes were monitored throughout surgical procedures to indicate the level of anaesthesia. The left adrenal gland was exposed and 5–10 μl Rhodamine Dextran Lysine (RDL, 10 %, Molecular Probes) injected into the adrenal medulla. The wound was sutured and animals allowed to recover for between 2 and 8 days.

Slice preparation

The methods used in obtaining whole-cell recordings from rat thoracic spinal cord slices have been described in detail previously (Logan *et al.* 1996). Briefly Sprague-Dawley rats (9–17 days old) were deeply anaesthetised with halothane and a laminectomy performed. A thoracic segment of spinal cord (T4–T12) was removed and the animal killed by decapitation. Spinal cord slices (400 μm thick) were cut using a vibratome (Leica VT1000S) and allowed to equilibrate for 1 h at room temperature in artificial cerebrospinal fluid (ACSF) of the following composition (mM): NaCl, 127; KCl, 1.9; KH_2PO_4, 1.2; $CaCl_2$ 2.4; $MgCl_2$, 1.3; $NaHCO_3$, 26; D-glucose 10; gassed with 95 % O_2–5 % CO_2; pH 7.4. A slice was subsequently transferred to a recording chamber of the sub-mersion type and continuously superfused with ACSF. In some experiments the ionic composition of the ACSF was manipulated. In experiments where low $[K^+]_o$ was used, KCl was omitted from the ACSF and KH_2PO_4 was replaced with equimolar NaH_2PO_4. Ca^{2+} was omitted and $MgCl_2$ concentration was increased to 5.2 mM when nominally zero Ca^{2+}-containing ACSF was required. A compromised sodium gradient was achieved by substitution of 67 mM NaCl with 67 mM Tris-HCl, giving a final Na^+ concentration of 60 mM. External pH was lowered by reducing $NaHCO_3$ to 8 mM and substituting with equimolar NaCl, giving a final external pH of 6.2.

Electrophysiological recordings

Whole-cell recordings were obtained from SPN at room temperature (18–21 °C) with patch pipettes of resistances 4–10 MΩ filled with the following solution (mM); potassium gluconate, 130; KCl, 10; Mg-ATP, 4; EGTA, 1; Hepes, 10; pH 7.4 with NaOH. In some experiments potassium conductances were blocked by Cs^+-loading cells. In these instances CsCl (140 mM) replaced potasssium gluconate and KCl. In some experiments QX-314 (4 mM, Alomone) was included in the pipette solution to block voltage-dependent sodium channels. Lucifer Yellow (dipotassium salt, 5 mg ml^{-1}, Sigma, see Spanswick *et al.* 1998) or Alexa 594 (50–100 μM, Molecular Probes) was included in the pipette solution to intracellularly label neurones from which recordings were made. Usually, only one neurone per slice was recorded. Recordings were obtained with a patch clamp amplifier (Axopatch-1D, Axon Instruments). Data acquisition and storage for subsequent off-line analysis was achieved with pCLAMP8 software (Axon Instruments).

Drugs were made up as concentrated stocks in distilled water, except for quinine, which was dissolved in ethanol. Drugs were subsequently diluted to the required concentration in ACSF prior to application. Immediately prior to experimentation, arachidonic acid was dissolved as a 20 mM stock solution in ethanol and subsequently added to ACSF to give final concentrations between 10 and 100 μM. Each arachidonic acid solution was vortexed and protected from light. Appropriate vehicle controls were carried out.

Double labelling of SPN

In spinal cord slices prepared from rats in which the adrenal medulla had been injected with RDL, cells were recorded on the ipsilateral side using a 'blind' approach. Following recording the slices were fixed in 4 % paraformaldehyde in phosphate buffer for 8–24 h and subsequently transferred to 25 % sucrose in phosphate buffer for 48 h. Slices were frozen and re-sectioned into 25–35 μm sections, collected on a glass slide and air dried. Sections were viewed under a fluorescent microscope (Zeiss Axioskop) with appropriate filters for Alexa 594, Lucifer Yellow and RDL, and either conventional slide photography or analogue image capture employed to develop permanent records.

Quantification of membrane properties

Resting membrane potential refers to the read-out from the amplifier and was corrected for junction potential offset (10 mV) after recording. The input resistance was determined by fitting the portion of the *I–V* curve around steady-state membrane potentials with a straight line. The time constant (τ) was evaluated by fitting the first membrane-voltage response to hyperpolarising current pulses (5–20 pA), with one or two exponential functions. The duration of the action potential was measured at one-third of peak amplitude, taken from threshold values.

RESULTS

Distribution of AD-SPN

Both transverse and longitudinal spinal cord slices were prepared to investigate the distribution of AD-SPN, revealed by the presence of RDL in the cytoplasm and proximal dendrites. In longitudinal slices, prelabelled cells were organised in a columnar fashion along the medial edge of the lateral funiculi, ipsilateral to the site of injection (Fig. 1*A*) between approximately T3 andT12, with distinct clusters of labelled cells most prominent around T7–T10. Occasionally labelled cells were observed in the lateral funiculi. However, no cells were found in the intercalated, central autonomic areas or in the spinal cord contralateral to the injected adrenal medulla. This distribution of labelled cells corresponds with previously described locations of AD-SPN (Strack *et al.* 1988). In transverse slices, labelling was observed in the lateral horn, again ipsilateral to the injection site. On average four or five 400 μm slices, corresponding to the regions where the highest levels of labelling had been identified (T7–T10), were retained for recording purposes.

Passive membrane properties

Data were obtained from a total of 54 neurones that were double labelled with Lucifer Yellow or Alexa 594 from the

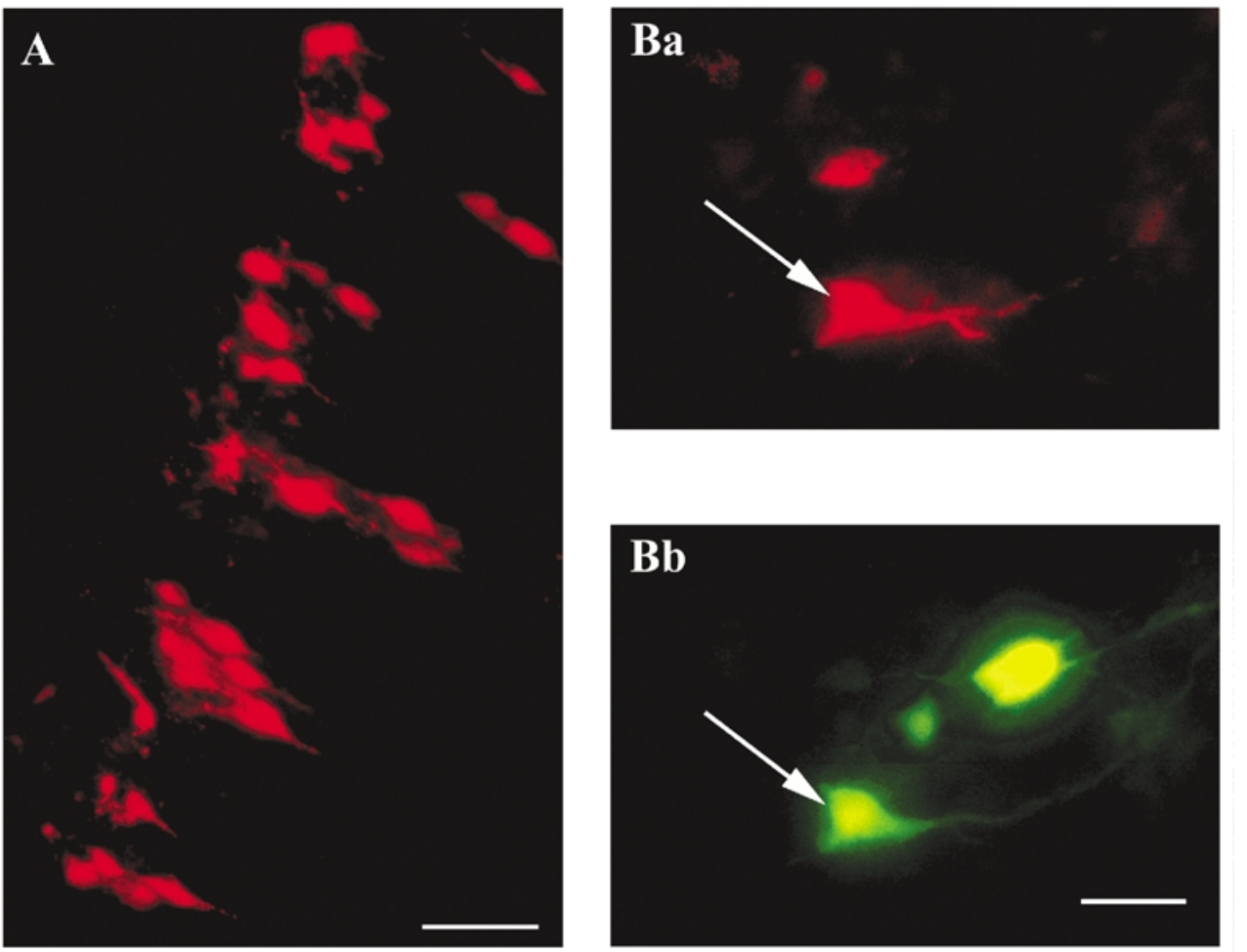

Figure 1. Intracellular and retrograde labels confirm recorded SPN innervate the adrenal medulla

A, longitudinal section of thoracolumbar spinal cord (35 μm thick) showing the distribution of SPN innervating the adrenal medulla as revealed by retrograde labelling of SPN with Rhodamine Dextran Lysine (RDL). All labelled SPN were observed in the spinal cord ipsilateral to the injected gland. *B*, transverse section (25 μm) of thoracic spinal cord showing SPNs labelled with RDL after injection into the adrenal medulla. The neurone indicated with the arrow in *a* was also filled (*b*) with Lucifer Yellow (LY) from the recording pipette, identifying its axonal projection to the adrenal medulla. In the latter section, note another LY-labelled neurone that lacked RDL, therefore not considered among the AD-SPN population data. Note, one neurone per slice was usually recorded except in instances to confirm the lack of overlap between the dyes used for retrograde and intracellular labelling. Scale bars are 50 μm in *A* and 25 μm *B*.

patch pipette and RDL from the adrenal medulla (Fig. 1*Ba* and *Bb*). Their basic membrane properties are summarised in Table 1 and the corresponding frequency histograms in Fig. 2*A*. The mean resting membrane potential was −62 ± 6 mV, ranging between −50 and −75 mV and showing a normal distribution. The mean input resistance was 410 ± 241 MΩ with a distribution slightly skewed towards higher resistances. A separate peak in the distribution suggests the possibility of a subgroup of neurones with a relatively low input resistance. The time constant (τ) was best estimated by fitting double exponentials to the membrane voltage charging curves induced by injection of small, hyperpolarising rectangular-wave current pulses (10–20 pA, 500 ms). The longest exponential was taken as τ. The mean τ of AD-SPN was 104 ± 53 ms, with a normal distribution between 44 and 194 ms.

Active membrane properties

Active membrane properties of AD-SPN were investigated by examination of the membrane responses to injection of current pulses (−200 to +20 pA, 1 s duration, 0.01 Hz) using potassium gluconate-based internal pipette solutions. The action potential of AD-SPN had a mean peak amplitude of 89 ± 15 mV and a duration measured at one-third peak amplitude of 5.7 ± 1.8 ms. In all AD-SPN, the action potential waveform was characterised by a distinct shoulder on the repolarisation phase (Fig. 2*B*a, inset). Under normal recording conditions, the majority of AD-SPN expressed two prominent active conductances that could be detected in response to injection of hyperpolarising current pulses from resting membrane potentials: an instantaneous inward rectification and a transient outward rectification (Fig. 2*B*).

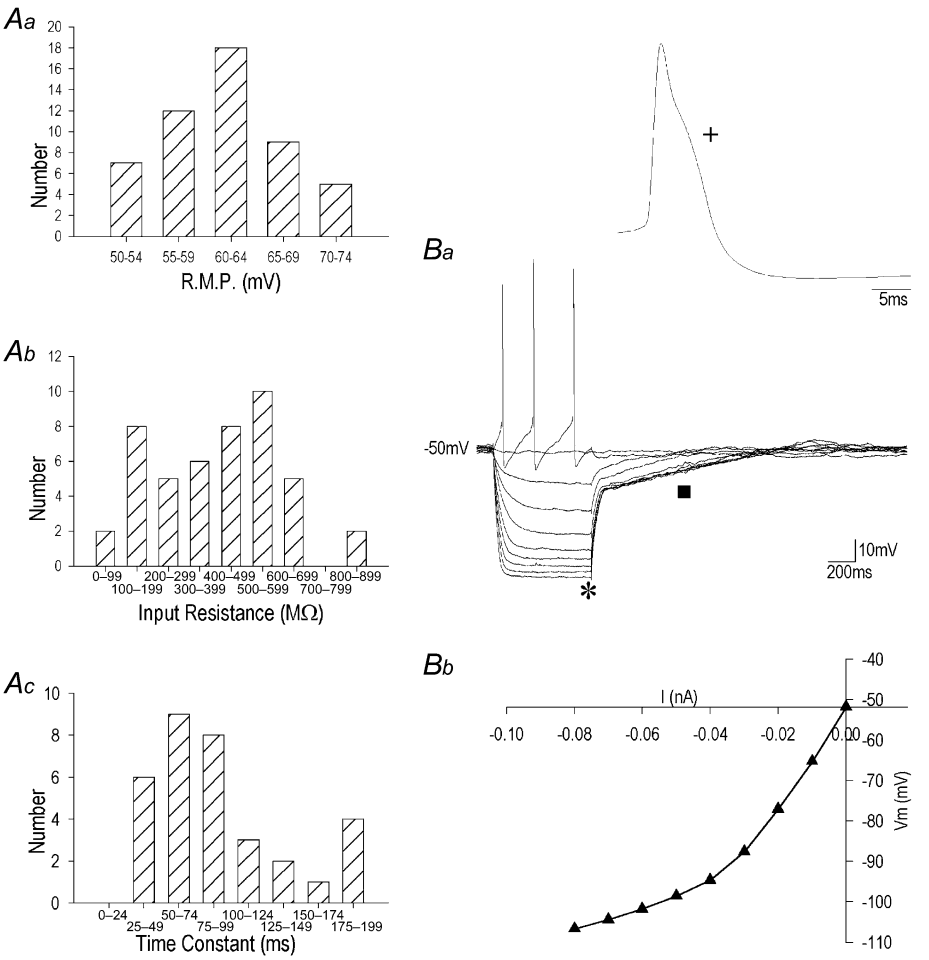

Figure 2. Membrane properties characteristic of AD-SPN

A, frequency histograms summarising the distribution of passive membrane properties of AD-SPN. *a*, resting membrane potentials (RMP; mV). *b*, input resistances (MΩ). *c*, membrane time constants (ms). *B*, whole-cell current-clamp recordings (holding potential −50 mV) illustrate characteristic active membrane properties. *a*, instantaneous inward rectification (*) activated during the membrane response to large amplitude hyperpolarising current pulses (not shown), and transient outward rectification (■) observed as a delayed return to rest of the membrane responses. Also shown in the inset is an action potential on a faster time base to illustrate the pronounced shoulder on the repolarising phase (+). *b*, a steady-state *I–V* curve plotted from data recorded at the end of membrane responses to current injection shown above reveals the inward rectification activated around −80 mV.

Table 1. Summary of membrane properties of SPN innervating the adrenal medulla

Membrane property		*n*
Resting membrane potential (mV)	−62.2 ± 5.7	54
Input resistance (MΩ)	410 ± 241	54
Action potential amplitude (mV)	88.5 ± 15.6	54
Action potential duration (ms)	5.7 ± 1.8	54
After-hyperpolarisation amplitude (mV)	25.9 ± 6.8	54
After-hyperpolarisation 90–10% decay time (ms)	297.7 ± 150.2	54
Presence of shoulder on action potential repolarisation phase	100 %	54/54
Presence of transient outward rectification	96 %	52/54
Presence of anomalous inward rectification	89 %	48/54

Whole-cell recordings were made from 54 SPN identified as innervating the adrenal medulla by the presence of a retrograde label, rhodamine dextran lysine (RDL) injected into the adrenal medulla and a second label Lucifer Yellow or Alexa 594 introduced from the recording electrode. The table summarises data obtained from these neurones. Results are expressed as means ± S.D. except for the descriptive data that are described as percentage of neurones that expressed a particular active conductance indicated in the table.

Inward rectification

AD-SPN exhibited a linear *I–V* relationship at steady-state membrane potentials between −50 and −80 mV. In the majority of AD-SPN (91 %), a fall in neuronal input resistance was observed from 410 ± 241 MΩ at membrane potentials close to rest to 138 ± 86 MΩ at membrane potentials more negative than around −80 mV (Figs 2*B* and 3, $n = 36$). This inward rectification was instantaneous, time independent, and was illustrated in the plots of voltage–current relations as a decrease in the gradient of the slope at negative membrane potentials (Fig. 3*B*).

To clarify the nature of this conductance, the effects of a range of ion channel blockers and ion substitutions were tested in the presence of TTX (0.5–1 μM). Manipulating the driving force for K^+ ions by superfusion of nominally 0 mM K^+ ACSF reduced the inward rectification (Fig. 3*C*), suggesting this conductance was mediated by a K^+ conductance. Bath application of Ba^{2+} (100 μM) completely

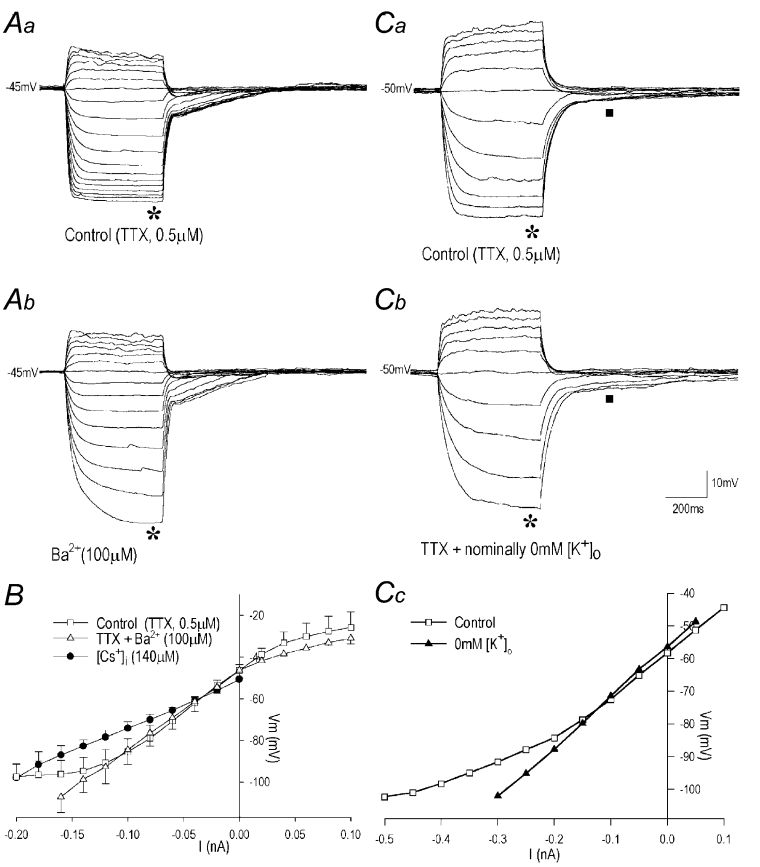

Figure 3. Instantaneous inward rectification in AD-SPN is mediated by a Ba^{2+}- and Cs^+-sensitive K^+ conductance

A, samples of voltage traces recorded in the presence of TTX (0.5 μM) illustrate membrane responses to injection of current pulses (−200 to 100 pA, 20 pA increments) from a holding potential of −45 mV. Note in *a* instantaneous inward rectification activated in response to large amplitude current pulses and in *b* its reduction in the presence of extracellular barium. *B*, steady-state *I–V* curves illustrate pronounced inward rectification in control (□) and its subsequent blockade in the presence of Ba^{2+} (△). Also note the absence of instantaneous inward rectification shown in an *I–V* curve for Cs^+-loaded neurones ($n = 12$, ●). *C*, voltage –current relations of an AD-SPN in the presence of 3.1 mM extracellular K^+ (*a*) and nominally zero K^+-containing ACSF (*b*). Membrane responses were evoked by injection of rectangular-wave current pulses (−120 to +100 pA, 20 pA increments, not shown) from a holding potential of −50 mV in the presence of TTX (0.5 μM). Note the enhanced transient outward rectification (■) and reduced instantaneous inward rectification (*) following the manipulation of the K^+ ion concentration gradient. The data plotted in *c* for the above illustrate instantaneous inward rectification (□) and its reduction in nominally zero K^+-containing bathing medium (▲).

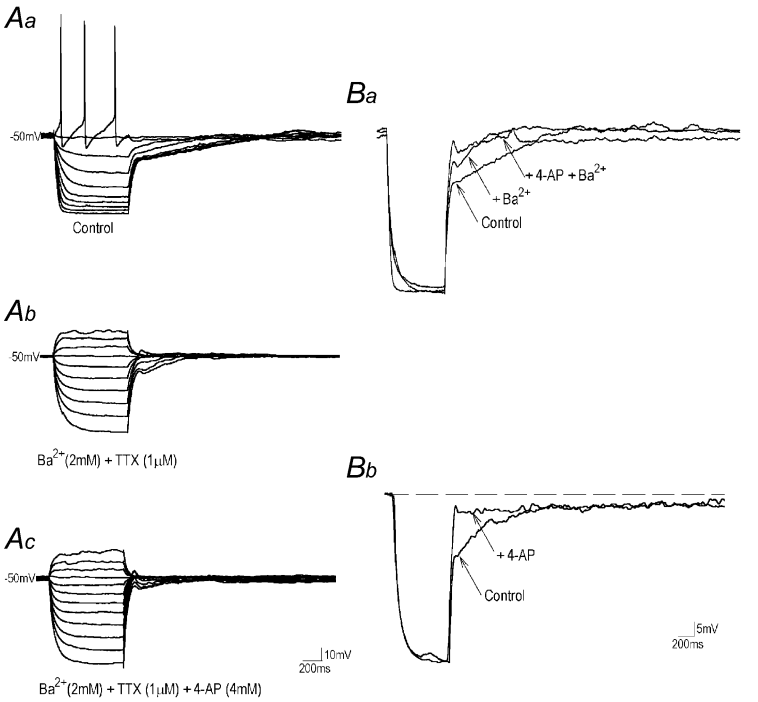

Figure 4. Sensitivity of the transient outward rectification to extracellular Ba^{2+} and 4-AP

A, voltage traces illustrate the transient outward rectification as a delayed return to the resting or holding potential at the break of the membrane response to hyperpolarising current pulses (20 pA steps) to the holding membrane potential (−50 mV; *a*); and its partial reduction in the presence of Ba^{2+}. Subsequent addition of 4-AP (*c*) reduced further the remaining transient outward rectification.
B, superimposed samples of membrane responses to hyperpolarising current pulses reveal the sensitivity of a slow component of the transient outward rectification to Ba^{2+} and a relatively fast component sensitive to subsequent addition of 4-AP (*a*). Traces in *b* illustrate the resistance of the slow component to 4-AP.

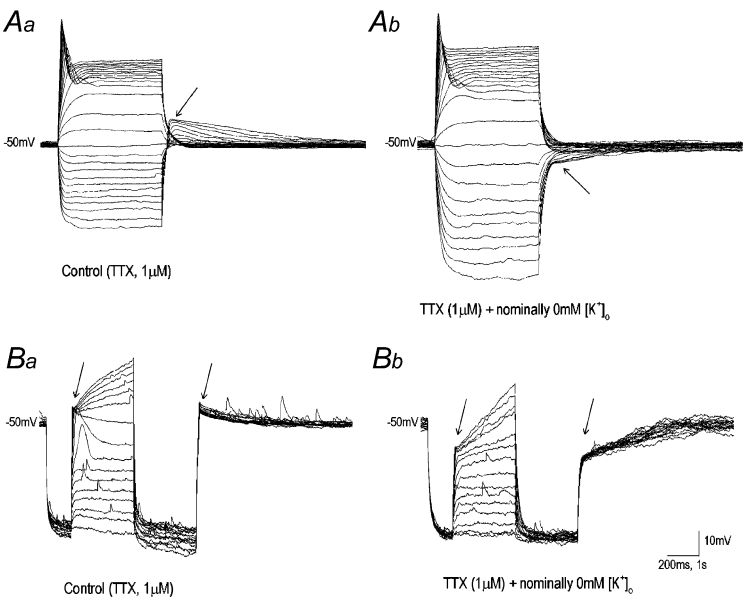

Figure 5. The transient outward rectification is insensitive to intracellular Cs^+

A, voltage–current relations of a SPN in which intracellular K^+ was replaced with equimolar Cs^+ (140 mM; *a*) and subsequently after reducing extracellular K^+ from 3.1 mM to nominally zero K^+-containing ACSF (*b*). Membrane responses were evoked by injection of rectangular-wave current pulses (−220 to +280 pA, 20 pA increments) in the presence of TTX (1.0 μM). Note the shift in polarity of the transient outward rectification in the presence of intracellular Cs^+ and its subsequent reversal in nominally zero K^+-containing ACSF (arrows). *B*, superimposed membrane responses to depolarising current pulses (20 pA steps) following removal of inactivation by hyperpolarising current injection (−200 pA) to membrane potentials around −100 mV in Cs^+-loaded SPN. In *a* note the transient depolarisation activated around −65 mV, delayed depolarisation around −45 mV and rebound depolarisation at the break of the response to the hyperpolarising step. In *b*, subsequent exposure of the slice to nominally 0 mM K^+-containing ACSF recovered a transient outward rectification activated at membrane potentials around −65 mV and at the offset of the membrane response to the hyperpolarising current injection.

blocked the instantaneous inward rectification in all neurones tested ($n = 6$; Fig. 3*A*). Neuronal input resistance following activation of the inward rectifier, over the membrane potential range −80 to −110 mV, increased from 87 ± 25 MΩ under control conditions to 409 ± 61 MΩ ($n = 6$) in the presence of Ba^{2+}. The reversal potential of the Ba^{2+}-induced block of this conductance was −96 ± 4 mV, close to the reversal potential for potassium ions under our recording conditions ($E_K = -96.2$ mV). Replacing intracellular K^+ with equimolar Cs^+ (140 mM) completely blocked the instantaneous inward rectifier ($n = 32$; Fig. 3*B*). Tolbutamide (10–200 μM; $n = 4$) was without effect on this conductance.

Transient outward rectification

The majority (97 %) of AD-SPN expressed a transient outward rectification (Fig. 3*A*), observed as a delayed return to rest of membrane responses (greater than around −10 mV from rest) to hyperpolarising current pulses (−60 to −140 pA, 500 ms, 0.01–0.1 Hz) (Figs 3*A* and *C*, 4*Aa* and *Ba*). At the break of the membrane response to hyperpolarising current pulse injections, this conductance was activated at a mean membrane potential of −63 ± 5 mV ($n = 36$). The transient outward rectifier was also observed in response to depolarising current pulses (80–180 pA, 2 s, 0.08–0.05 Hz) from relatively negative resting or holding potentials (>−70 mV), thus manifesting as a delay in the time to achieve threshold for firing. The mean τ was 3555 ± 903 ms ($n = 12$), considerably longer than the membrane τ, suggesting the presence of an active conductance. In nominally 0 mM K^+, ACSF transient outward rectification was enhanced (Fig. 3*C*), suggesting mediation by K^+ ions.

Using K^+ channel blockers, the transient outward rectification could be separated into two components (Fig. 4). Bath application of Ba^{2+} (2 mM; $n = 4$; Fig. 4*A* and *B*) reduced, but did not completely block, the transient outward rectification. The Ba^{2+}-sensitive component was of long duration with a τ of 3272 ± 673 ms and amplitude of 6 ± 2 mV ($n = 4$), measured relative to a resting or holding potential of −50 mV. In the presence of Ba^{2+} (2 mM) a relatively fast component of the outward rectification persisted, having a mean peak amplitude (estimated relative to the resting or holding potential) of 8 ± 2 mV and τ of 435 ± 133 ms ($n = 3$). This fast component was reduced by 4-AP (2–4 mM; $n = 8$; Fig. 4*Ac* and *B*). Both the Ba^{2+} and 4-AP-sensitive components were insensitive to TEA (30 mM, $n = 4$), Co^{2+} (2 mM, $n = 3$), Ni^{2+} (2 mM, $n = 4$), Cd^{2+} (100 μM, $n = 2$) or quinine (100 μM, $n = 5$).

The effects of intracellular Cs^+ were tested on the outward rectification. Replacing intracellular K^+ with equimolar Cs^+ (140 mM) revealed a rebound depolarisation at the offset of the membrane response to hyperpolarisation (Fig. 5*A*, $n = 6$) or a transient depolarisation in response to depolarising current pulses from a relatively negative holding potential (−80 to −100 mV; Fig. 5*B*). The mean peak amplitude of this potential, measured relative to the resting or holding potential of −50 mV, was 14 ± 3 mV with a τ of 528 ± 101 ms ($n = 6$), close to that observed for the 4-AP-sensitive transient outward rectification. Shifting the driving force for K^+ ions by superfusion of nominally 0 mM K^+-containing ACSF reversed the polarity of the depolarising shift, restoring transient outward rectification

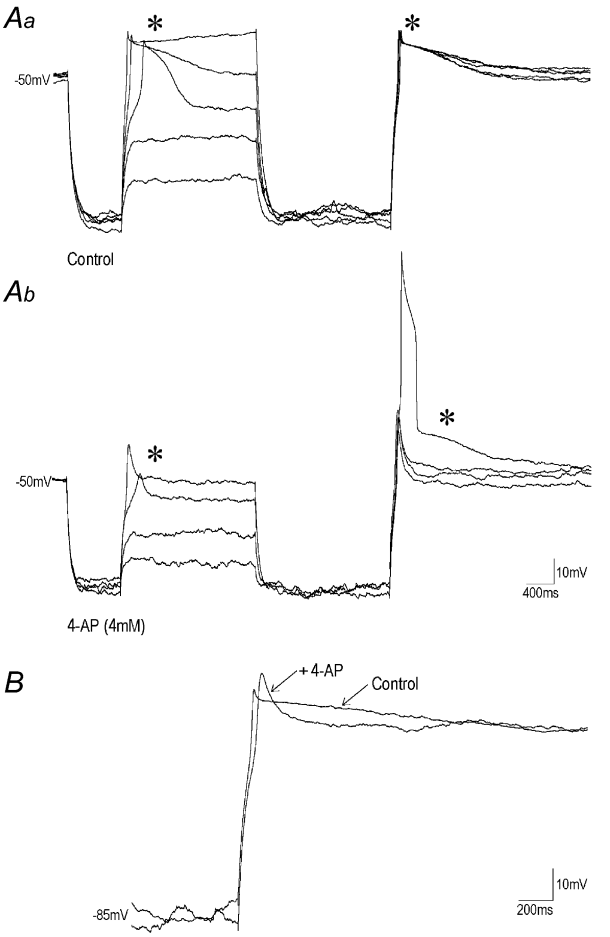

Figure 6. Two distinct components mediate the rebound depolarization revealed in Cs^+-loaded AD-SPN

A, superimposed membrane responses to depolarising current pulses (20 pA steps) following removal of inactivation by hyperpolarising current injection (−200 pA) to membrane potentials around −100 mV in Cs^+-loaded SPN. In *a* note the depolarisation activated around −65 mV and rebound depolarisation at the break of the response to the hyperpolarising step. * In *b*, subsequent application of 4-AP (4 mM) revealed a smaller more transient depolarisation activated around −55 to −60 mV and transient rebound depolarisation at the break of the response to membrane hyperpolarisation which could give rise to firing *. *B*, superimposed records showing the rebound depolarisations evoked at the offset of the membrane response to hyperpolarisation. Note the transient nature of the rebound depolarisation in the presence of 4-AP compared with control.

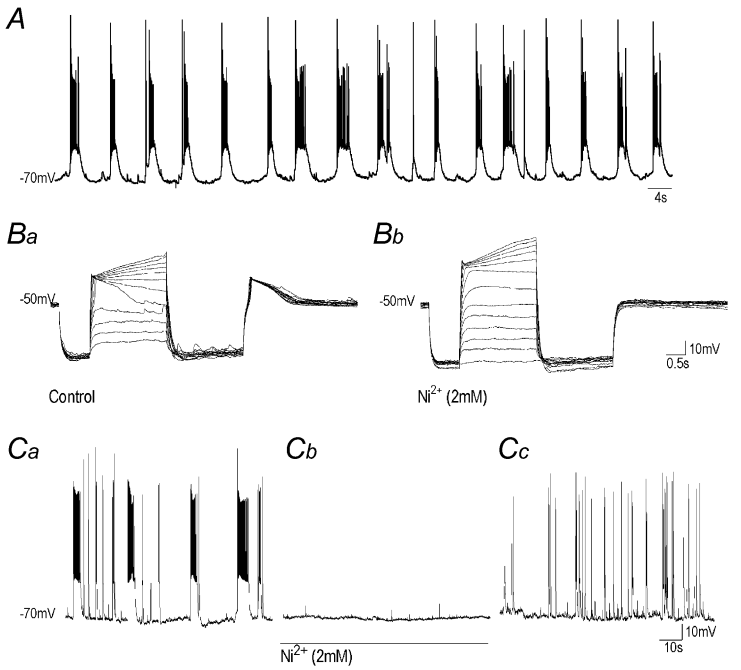

Figure 7. Burst firing induced in Cs^+-loaded AD-SPN is mediated by a Ni^{2+}-sensitive low-threshold Ca^{2+} conductance

A, spontaneous burst firing pattern of activity in Cs^+-loaded AD-SPN. *B*, superimposed membrane responses to depolarising current pulses (20 pA steps) following removal of inactivation by hyperpolarising current injection (−100 pA) to membrane potentials around −100 mV in Cs^+-loaded AD-SPN. In *a*, note the low-threshold depolarisation activated around −50 mV and rebound depolarisation at the break of the response to the hyperpolarising step. In *b*, note the transient depolarisation was completely blocked by subsequent exposure to Ni^{2+}. *C*, spontaneous activity in Cs^+-loaded AD-SPN (*a*) was completely (*b*) reversibly (*c*) blocked by Ni^{2+}.

($n = 4$; Fig. 5). The rebound depolarisation in Cs^+-loaded SPN was sensitive to 4-AP (2–4 mM) in all neurones tested ($n = 5$; Fig. 6) and insensitive to extracellular Cs^+ (2 mM, $n = 2$) and Ba^{2+} (2 mM, $n = 3$). The insensitivity of the conductance to Ba^{2+} in Cs^+-loaded SPN suggests that the slow component of outward rectification, observed with potassium-based intracellular solutions, was blocked by intracellular Cs^+, unlike the 4-AP-sensitive component.

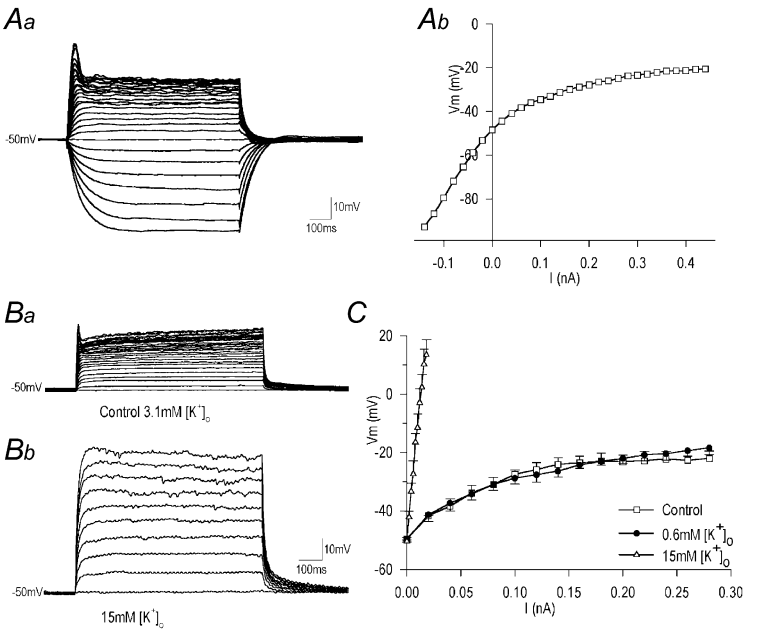

Figure 8. A sustained voltage-dependent outward rectifying K^+ conductance in AD-SPN

A, samples of a continuous whole-cell current-clamp recording illustrate superimposed membrane responses to injection of current pulses in the presence of 4-AP, TEA, Co^{2+} and TTX (1 μM; *a*). Note the persistent outward rectification in response to depolarising current pulses observed under these recording conditions. In the plot of these data (*b*), note the decrease in slope conductance at membrane potentials less negative than around −40 mV. *B*, superimposed membrane responses showing voltage–current relations of a AD-SPN in the presence of 3.1 mM extracellular K^+ (*a*) and subsequently in elevated extracellular K^+ (15 mM; (*b*)). Membrane responses were evoked by injection of depolarising current pulses (10 pA steps in *a*, 2 pA steps in *b*) in the presence of TTX (1 μM), TEA (30 mM), Ni^{2+} (2 mM) and 4-AP (4 mM). Note the strong outward rectification in control was reduced following exposure to elevated extracellular K^+. *C*, plot of data shown in *B* and from data recorded in the same cell in reduced extracellular K^+ (0.6 mM).

Low-threshold calcium conductance

In Cs^+-loaded neurones in the presence of 4-AP (4 mM) and TTX (1 μM), a rebound excitation persisted (Fig. 6, $n = 31$). This conductance was activated at the offset of the response to hyperpolarising current injection (−60 to −140 pA, 500 ms, 0.01–0.1 Hz), in response to depolarisation from a relatively negative holding potential, or in response to depolarising current injection following a hyperpolarising prepulse driving the membrane potential to around −85 to −100 mV (Fig. 6). The rebound excitation, characterised by a rapid depolarisation followed by a slower decay, activated at around −77 ± 4 mV and had a mean peak amplitude of 28 ± 7 mV and a half-time to decay of 441 ± 210 ms ($n = 10$). The low-threshold calcium channel blocker Ni^{2+} completely blocked the rebound excitation at a concentration of 1–2 mM ($n = 3$; Fig. 7*B*), but was without effect at a concentration of 100 μM ($n = 5$).

Cs^+ (140 mM)-loading SPN induced a spontaneous burst firing pattern of activity in 23 of 31 SPN (Fig. 7*A* and *C*). From resting membrane potentials between −70 and −55 mV, bursts of activity were characterised by rapid depolarising shifts that reached threshold for action potential firing, followed by a slower return to baseline membrane potentials. The mean frequency of these bursts was 0.6 ± 0.2 Hz (range 0.1–1.5 Hz) with the depolarising phases or shifts lasting 1.5–5 s, interspersed with silent periods. The number of action potentials superimposed on the depolarised shifts varied from one to 15. In all three neurones tested, Ni^{2+} (2 mM) completely and reversibly blocked all activity (Fig. 7*C*).

High-threshold calcium spike

In the presence of TTX (0.5–1 μM), the low-threshold calcium conductance could give rise to an action potential, with mean peak amplitude and duration measured at one-third of peak amplitude of 92 ± 13 mV and 20 ± 6 ms, respectively. Superfusion of nominally Ca^{2+}-free ACSF (substituted with 5.2 mM $MgCl_2$; $n = 6$), Cd^{2+} (100 μM, $n = 6$) or Ni^{2+} (2 mM, $n = 4$) blocked the high-threshold spike.

Sustained outward rectification

In the presence of TTX (0.5–1 μM) and following block of Ca^{2+} conductances with Cd^{2+} (100 μM) or Ni^{2+} (2 mM), a sustained outward rectification could be activated at membrane potentials positive to around −35 mV in all

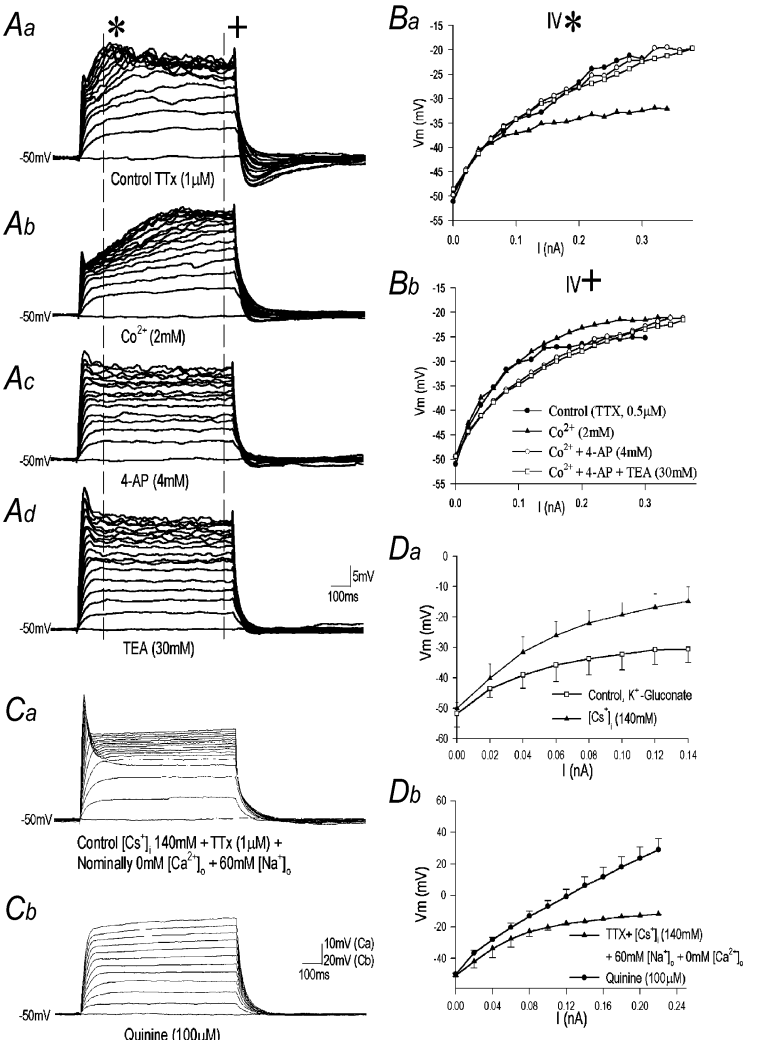

Figure 9. The effects of ion channel blockers on the sustained outward rectification

A, effects of ion channel blockers and ion substitutions on outward rectification evoked in response to membrane depolarisation from holding potentials around −50 mV. Superimposed membrane responses to depolarising current pulses (10 pA steps, *a*), revealed a transient early outward rectification leading to a delay to the peak of the membrane response, and a sustained rectification at the peak of the membrane response. In the presence of Co^{2+}, the transient rectification was more obvious (*b*), whereas its subsequently blockade by 4-AP (*c*) left a sustained outward rectification. In *d*, high concentrations of TEA partly reduced the outward rectification, but sustained outward rectification remained. *B*, plots of data shown in *A* measured at the peak of the membrane response in control and at the same time point for subsequent manipulations (*), and during the steady-state membrane response (+). *C*, sustained outward rectification persisted when intracellular K^+ was exchanged for equimolar Cs^+ (*a*), in nominally 0 mM extracellular Ca^{2+} and reduced extracellular Na^+, but was completely blocked by quinine (*b*). *Da*, pooled data from *I–V* plots showing the effects of intracellular Cs^+ on outward rectification compared with control recording conditions with K^+-gluconate-based pipette solution ($n = 12$); *b*, pooled data illustrate the effects of quinine on sustained outward rectification ($n = 4$).

neurones tested (Fig. 8*A*, $n = 19$). Step depolarisations (10–300 pA, 600 ms, 0.2 Hz) from a membrane potential of −50 mV induced a fall in input resistance from 325 ± 194 MΩ, close to the resting or holding potential, to 48 ± 38 MΩ at potentials between −35 and −15 mV. This outward rectification was sustained over the time course of the depolarising current pulse injection (up to 600 ms) and showed little indication of inactivation. The sustained outward rectification was illustrated in plots of the voltage–current relations by a decrease in the gradient of the slope at depolarised membrane potentials (Fig. 8*Ab*).

To identify the nature of the ions mediating this conductance, the effects of changes in extracellular ion concentrations were investigated. Manipulating the driving force for K^+ ions by reducing extracellular K^+ concentration from 3.1 to 0.6 mM ($n = 15$) had no significant effect. However, increasing extracellular K^+ concentration from 3.1 to 15 mM ($n = 4$) markedly reduced the outward rectification (Fig. 8*B*). When intracellular K^+ was replaced with equimolar Cs^+ a sustained outward rectification persisted ($n = 31$; Fig. 9*Ca* and *D*) that was insensitive to changes in Ca^{2+}, Na^+ and Cl^- ion concentration gradients. These data suggest that a component of sustained outward rectification in AD-SPN is mediated through Cs^+-permeable K^+ channels.

To characterise further the nature of this conductance, we tested a range of agents and manipulations known to affect K^+ channels. Bath applications of muscarine (40 μM, $n = 2$), 4-AP (4 mM; $n = 17$; Fig. 9*Ac*), TEA (30 mM; $n = 12$; Fig. 9*Ad*), Ba^{2+} (2 mM, $n = 9$), Ni^{2+} (2 mM; $n = 7$; Figs 10*A*), Co^{2+} (2 mM; $n = 4$; Fig. 9*Ab*) or Cd^{2+} (100 μM; $n = 7$) were without significant effect (see Fig. 9). However, the outward rectification was completely blocked by quinine ($n = 5$; Fig. 9*C*). Two further manoeuvres significantly affected this component of the sustained outward rectification. First, lowering extracellular pH from 7.4 to 6.2 partly reduced the sustained outward rectification at membrane

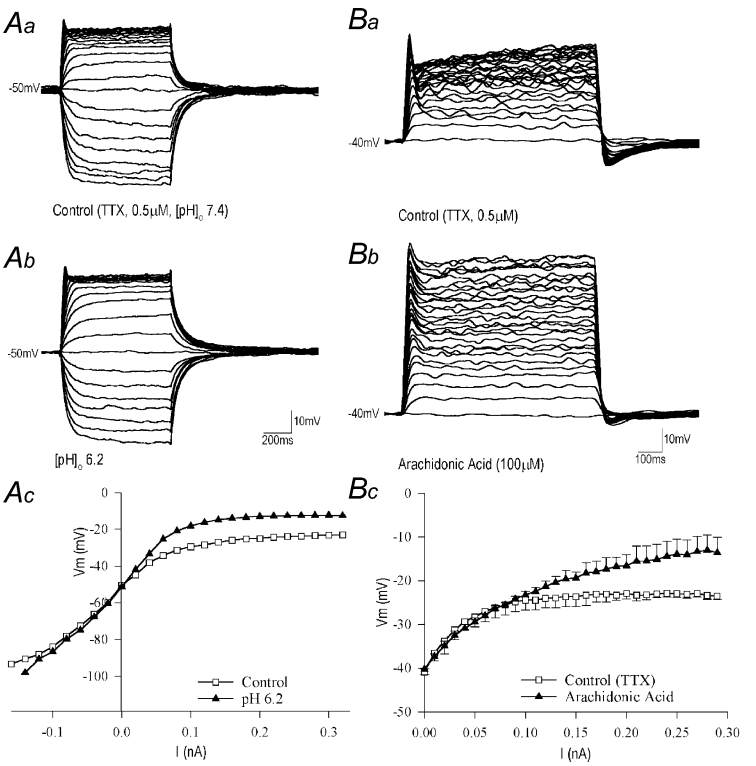

Figure 10. The effects of changes in extracellular pH and arachidonic acid on the sustained outward rectification

A, samples of a continuous whole-cell current-clamp record, in the presence of TTX (0.5 μM), showing membrane responses to injection of current pulses (10 pA increments) from a holding potential of −50 mV. Membrane depolarisation evoked a sustained outward rectification (*a*) at pH 7.4. Reducing extracellular pH to 6.2 increased neuronal input resistance at potentials less negative than around −40 mV. At potentials less negative than around −25 mV a sustained outward rectification persisted (*b*). *c*, plot of data shown above: extracellular pH 7.4 (□) and pH 6.2 (▲). *B*, sustained outward rectification was sensitive to arachidonic acid. Membrane depolarisation evoked a sustained outward rectification (*a*)that was reduced in the presence of arachidonic acid (100 μM) (*b*). Membrane responses were evoked by depolarizing current pulses (10 pA steps) from holding potentials of −40 mV, in the presence of TTX (1 μM), Ni^{2+} (2 mM) and 4-AP (4 mM) to block voltage-dependent sodium, low-threshold calcium and transient outward rectification respectively. *C*, plot of pooled data from three neurones to illustrate the effects of arachidonic acid on the outward rectification: control (□); arachidonic acid (▲).

potentials between −30 and −15 mV, although a prominent rectification persisted at membrane potentials less negative than around −15 mV ($n = 4$, Fig. 10*A*). Neuronal input resistance increased from 145 ± 42 MΩ at pH 7.4 to 383 ± 132 MΩ at pH 6.2 during activation of the sustained outward rectification, corresponding to a 265 % increase. These effects were reversible on returning the bathing medium to pH 7.4. Second, bath application of arachidonic acid (100 μM) also markedly suppressed a component of the outward rectification in all neurones tested ($n = 4$, Fig. 10*B*). These effects of arachidonic acid were slow in onset and irreversible over the time course of recording. Neuronal input resistance during activation of the sustained outward rectification, at potentials positive to −25 mV, increased from 14 ± 3 to 83 ± 39 MΩ in the presence of arachidonic acid, corresponding to a 580 % increase.

Effects of ion channel blockers on the action potential

Experiments outlined above identified two outwardly rectifying potassium conductances in AD-SPN: a transient outward rectification activated at the offset of the membrane response to hyperpolarising current pulses; and a sustained outward rectification observed at membrane potentials less negative than around −35 mV. A functional role for these conductances was investigated by examining the effects of ion channel blockers on action potentials and associated after-hyperpolarisations (AHP) evoked either by antidromic stimulation or by direct current injection through the recording pipette. In all six neurones tested with 4-AP (4 mM), a transient outward rectifier blocker, the repolarising phase of the action potential was prolonged and the duration (measured at one-third peak amplitude) increased from 3.8 ± 0.5 ms under control conditions to 10.6 ± 3.9 ms**.** Concomitant with this broadening of the action potential was a significant reduction in the AHP, from a mean peak amplitude and τ of 13 ± 1 mV and 151 ± 55 ms under control conditions to 6 ± 2 mV and 95 ± 34 ms, respectively ($n = 6$). As 4-AP can exert effects on other potassium channel species, the effects of 4-AP were tested in the presence of Ba^{2+} (2 mM, $n = 2$) or TEA (30 mM, $n = 2$), to block other outward currents expressed in SPN (Miyazaki *et al.* 1996). The action potential repolarisation was significantly slowed (Fig. 11*Aa*), with the duration increasing from 3.2 ± 0.4 ms in control conditions to 6.8 ± 1.3 ms in the presence of Ba^{2+} or TEA ($n = 4$). Subsequent addition of 4-AP further increased the duration of the action potential to 12.4 ± 3.3 ms. Corresponding AHPs were reduced in the presence of 4-AP compared with the AHP evoked in the presence of TEA (Fig. 11*Ab*). The mean peak amplitude and duration of the AHP in the presence of TEA was reduced from 13.1 ± 0.9 mV and 151.0 ± 55.0 ms to 6.5 ± 1.9 mV and 94.6 ± 34.2 ms, respectively, in the presence of 4-AP ($n = 5$).

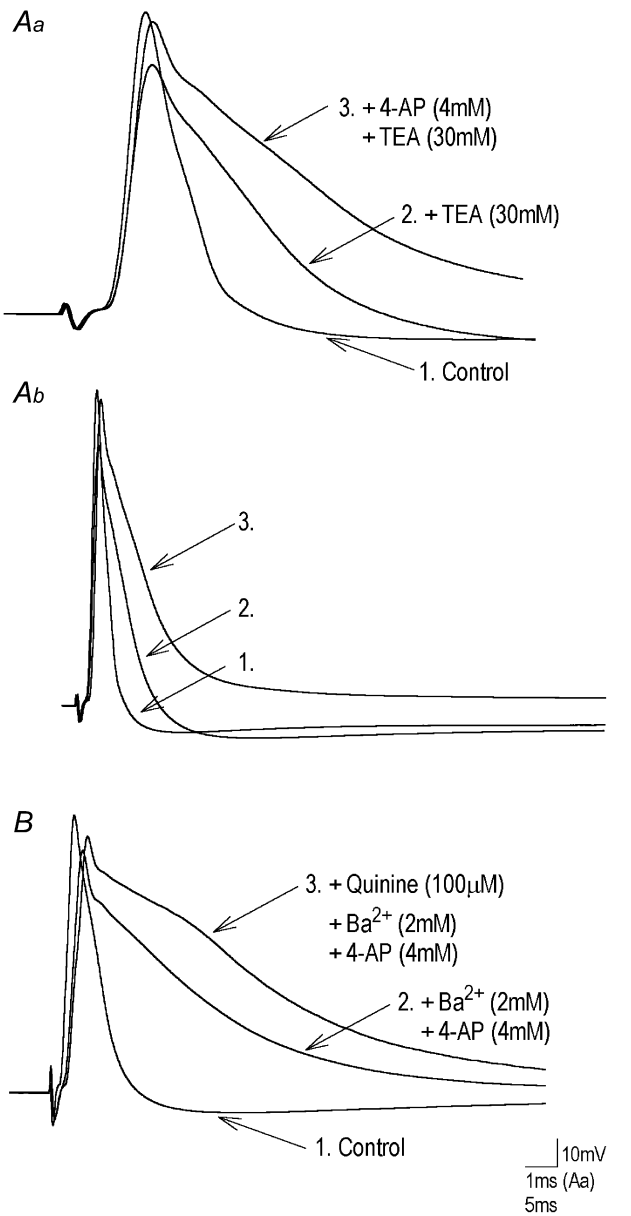

Figure 11. The role of outwardly rectifying conductances in action potential repolarisation and after-hyperpolarisation

Samples of a continuous whole-cell current-clamp recording illustrate the effects of ion channel blockers on the action potential and after-hyperpolarisation (AHP) waveforms. Each record is the average of 10 antidromic action potentials evoked by stimulation (9 V, 5 ms, 0.05 Hz) of the ventral horn exit zone. All records were obtained in the presence of D-AP5 (10 μM), NBQX (5 μM), bicuculline (10 μM) and strychnine (2 μM) to block fast chemical synaptic transmission. *A*, the evoked antidromic spike (1) was prolonged in the presence of 30 mM TEA (2) and further prolonged in the presence of both TEA and 4 mM 4-AP (3). In *b*, the same data as above but shown on a slower time base to illustrate the reduction in the AHP in the presence of TEA and 4-AP (3). *B*, recordings from another AD-SPN showing the effects of quinine on spike repolarisation. The evoked antidromic spike (1) was prolonged in the presence of 2 mM Ba^{2+} and 4 mM 4-AP (2) and further prolonged when 100 μM quinine was added in addition (3).

Next we investigated the role of the quinine-sensitive sustained outward rectifier. In all neurones tested ($n = 3$), the action potential duration increased from 2.8 ± 0.5 ms under control conditions to 4.5 ± 1.1 ms in the presence of quinine. To isolate the quinine-sensitive component we included Ba^{2+} and 4-AP, or TEA and 4-AP, in the bathing medium to block other components of the sustained outward rectification reported for SPN (Miyazaki *et al.* 1996). Under these conditions, the duration of the action potential increased to 8.4 ± 3.4 ms. Subsequent addition of quinine further increased the duration to 15.4 ± 6.3 ms (Fig. 11*B*, $n = 4$).

DISCUSSION

Data presented here are the first attempt to define intrinsic passive and active membrane properties involved in regulating excitability of SPN that innervate the catecholamine-secreting chromaffin cells of the adrenal medulla.

The mean resting membrane potential of AD-SPN was within the range of values previously reported for SPN in neonatal rats using similar techniques (Pickering *et al.* 1991; Logan *et al.* 1996). However, it should also be noted that the higher values for input resistance and action potential duration were probably overestimated, reflecting recording at lower temperatures rather than the improved electrode–membrane seals as has previously been suggested for SPN (Pickering *et al.* 1991). At physiological temperatures both action potential duration and input resistance are reduced compared with recordings at lower temperatures in SPN (authors' unpublished observations) and other central neurones (e.g. see Griffin & Boulant, 1995). Although the input resistance of AD-SPN had a distribution slightly skewed towards higher values, a separate peak in this distribution suggests the possibility of a subgroup of neurones with a relatively low input resistance. In relation to this, a subpopulation of SPN have been already characterised by low input resistance, reflecting electrotonic coupling (Logan *et al.* 1996; Nolan *et al.* 1999). Over the course of the present study we have identified a population of AD-SPN that are electrotonically coupled; they are the subject of a separate publication. Our awareness of this coupled population prompted us to use current rather than voltage-clamp recordings throughout this study.

In terms of their active membrane conductances AD-SPN constitute a relatively homogeneous population. However, the diversity of these conductances endows AD-SPN with an output that is dynamic and complex. This capability may be crucial for regulating catecholamine release in response to physiological and environmental demands.

Transient outward rectification in AD-SPN

AD-SPN expressed a transient outward rectification that was composed of two distinct potassium conductances: a fast component with a time constant of decay of 435 ± 133 ms and a slower component with a time constant of decay of 3555 ± 903 ms. The fast component was sensitive to 4-AP, changes in extracellular and intracellular K^+ ion concentration but insensitive to extracellular Ba^{2+} and TEA. Of note was its insensitivity to intracellular Cs^+, Cs^+ failing either to block or readily permeate these channels. This 4-AP-sensitive transient outward rectification is reminiscent of the A-type conductance previously described in SPN in adult cat (Dembowsky *et al.* 1986; Yoshimura *et al.* 1987*a*), guinea-pig (Inokuchi *et al.* 1993), neonatal rat (Miyazaki *et al.* 1996; Pickering *et al.* 1991) and other central neurones (see Rogawski, 1985). The insensitivity of the conductance to concentrations of 4-AP of less than 100 μM indicates that the conductance is an A- rather than D-type transient-outward rectification. The A-type transient rectifier in SPN has a longer duration than that previously reported for I_A in other CNS regions. Furthermore, 4-AP up to 4 mM blocks only the relatively fast component in SPN described here and previously (Pickering *et al.* 1991; Miyazaki *et al.* 1996). Similar conductances with longer activation and inactivation kinetics than I_A have been identified in neurones, including magnocellular cells in culture and slices (Cobbett *et al.* 1989; Li & Ferguson, 1996). The unusual time course of the A-conductance in AD-SPN may reflect the expression of Kchip (KCNIP1–4) subunits, a gene family contributing Kv4β-subunits of A-channels. The potentials for activation, the slowing of inactivation and rate of recovery from inactivation are dependent on Kchip gene expression and the presence of the Kchip splice variant (An *et al.* 2000; Bahring *et al.* 2001). A-type potassium conductances contribute to early spike repolarisation, delaying the onset of threshold and to regulation of repetitive firing (see Rogawski, 1985; Storm, 1990). Voltage-clamp recordings from SPN suggest A-channels are released from inactivation by hyperpolarisation and activated by depolarisation, and act to control firing frequency together with I_{AHP} (Miyazaki *et al.* 1996). Experiments described here, showing the effects of 4-AP on the action potential waveform under conditions where other conductances are blocked, suggest the A-type conductance acts to regulate firing frequency in AD-SPN partly due to a role in regulating spike repolarisation and partly by contributing to the AHP.

A second, pharmacologically distinguishable, slower component of transient outward rectification identified in AD-SPN was blocked by high concentrations of Ba^{2+} and intracellular Cs^+ and was separable from the A-conductance by its insensitivity to 4-AP. The prolonged time course of this transient rectification relative to the A-conductance is reminiscent of the D-conductance, a conductance that inactivates slowly below spike threshold over a time course of seconds and gives rise to a prolonged delay in the onset to firing (see Storm, 1990). Functionally, this is thought to allow different inputs to be temporally integrated (Storm,

1990). The potentials over which this slow outward rectification was activated would also be consistent with a similar role, and a role in regulating firing frequency by contributing to the AHP which is prolonged and lasts several seconds in SPN (Yoshimura *et al.* 1986*a*).

Sustained outward rectification in AD-SPN

Rectification in response to depolarising current pulses injected from resting membrane potentials has been observed with intracellular recordings from SPN in T1–T3 of spinal cord slices from adult cats (Yoshimura *et al.* 1986*b*). Voltage-clamp studies of SPN in the neonate rat have demonstrated three components of slow outward rectification in response to depolarising step commands: a delayed rectifier (I_K), a Ca^{2+}-dependent transient current (I_C) and a Ca^{2+}-dependent sustained current (I_{AHP}) (Miyazaki *et al.* 1996). These conductances are proposed to mediate, in part, spike repolarisation and the AHP. Outward rectification has been reported to be completely abolished by TEA in SPN (Miyazaki *et al.* 1996).

In AD-SPN, we describe a component of outward rectification that is insensitive to TEA, has unusual pharmacology and plays a role in spike repolarisation. This component of outward rectification, observed in all AD-SPN in response to depolarising current pulses, was activated at potentials positive to around −35 mV and was sensitive to quinine, changes in pH and arachidonic acid, but insensitive to 4-AP, Ba^{2+} and Ca^{2+} influx. This conductance was selectively sensitive to changes in K^+ ion and insensitive to changes in Na^+, Cl^- and Ca^{2+} ion concentration gradients, indicating mediation via K^+-selective ion channels. However, the outward rectification persisted in recording conditions where K^+ was replaced with Cs^+ in the recording pipette, suggesting that this conductance can also be carried by Cs^+ ions. Whereas Cs^+ permeability is not a common feature of K^+ channels, several voltage-clamp studies have reported Cs^+ permeability of outwardly rectifying, slowly inactivating currents in the subthalamic nucleus (Wigmore & Lacey, 2000), avian nucleus magnocellularis (Rathouz & Trussell, 1998), dorsal root ganglion (Trequattrini *et al.* 1996) and bullfrog sympathetic neurones (Block & Jones, 1997). Outwardly rectifying potassium conductances and corresponding currents are generally blocked by TEA, $Ba^{2+}$and 4-AP (e.g. see Wigmore & Lacey, 2000). Although insensitive to a range of K^+ channel blockers, the outward rectification described in AD-SPN was sensitive to quinine. Quinine has been shown to block a range of potassium currents, including those mediated by two-pore domain potassium channels (2PDKCs) in mammals (e.g. see Meadows & Randall, 2001), an inactivating A-current, non-inactivating M-current and a slowly inactivating delayed rectifier (I_K) in bullfrog sympathetic neurones (Imai *et al.* 1999). The quinine-sensitive outward rectification was also sensitive to a reduction in extracellular pH and arachidonic acid. Both changes in pH (see Tombaugh & Somjen, 1996; Traynelis, 1998; Rajan *et al.* 2000) and arachidonic acid (Colbert & Pan, 1999; Casavant *et al.* 2000; Holmqvist *et al.* 2001) have been shown to modulate a range of ion channels. Therefore, the pharmacology of sustained outward rectification in AD-SPN has similarities with aspects of other voltage-dependent and -independent K^+ channels. However, we are unaware of any direct correlation with previously reported outward rectifying conductances in neurones.

Our observations suggest AD-SPN express a novel potassium conductance permeable to Cs^+ and sensitive to quinine, extracellular pH and arachidonic acid. This conductance is important in mediating spike repolarisation in AD-SPN. These data indicate spike repolarisation in SPN to be complex, involving several separate K^+ conductances.

The inward rectifier

Membrane hyperpolarisation evoked an inward rectification in virtually all AD-SPN. This inward rectification was instantaneous, time independent and activated around −80 mV. The instantaneous inward rectification was blocked by Ba^{2+} and selectively mediated by K^+ ions. The conductance is therefore similar to the instantaneous or anomalous inward rectification previously described in SPN and other central neurones (Dembowsky *et al.* 1986; Pickering *et al.* 1991; Miyazaki *et al.* 1996). The functional role of this inward rectification in SPN and central neurones is unclear. Although suggested to contribute to spike after-hyperpolarisation in some neurones including SPN (Miyazaki *et al.* 1996), we consider this unlikely given the negative membrane potential at which it is activated. Similarly, a role in contributing to the resting membrane potential is unlikely given the resting membrane potentials of AD-SPN and the potential range over which the conductance was activated. One possibility is that the conductance acts to maintain the membrane potential within an operational window or readily excitable state, hence preventing neurones from becoming 'too hyperpolarised' and hence outside of that window.

Low-threshold calcium conductance revealed in AD-SPN

Block of K^+ conductances by Cs^+ loading of cells revealed a rebound excitation at the break of the membrane response to hyperpolarising current pulses, and a tendency for autorhythmicity. Both were sensitive to Ni^{2+}. This suggests AD-SPN express functional low-voltage-activated (LVA) T-type calcium conductances that underlie rhythmic burst firing patterns of activity. Although the concentrations of Ni^{2+} required to block the rebound excitation in AD-SPN were relatively high (>100 μM), other studies have shown considerable variation in the sensitivity of T-type Ca^{2+} conductances to this divalent cation (Lee *et al.* 1999). This is considered in part to reflect the subunit composition of

these channels. At the molecular level, the T-type channel family presently consists of three members: $Ca_V3.1$, $Ca_V3.2$ and $Ca_V3.3$ (see Perez-Reyes, 1999). Differential expression of these subunits and putative associated subunits can yield channels and conductances with distinct properties that may be tailored to specific neuronal functions. T-type channels are activated at potentials negative to threshold for Na^+-dependent action potential firing and activation of high-threshold Ca^{2+} conductances. Thus, in providing a depolarising drive, they act to amplify subthreshold stimuli leading to suprathreshold activity (see Huguenard, 1996). These features of T-type calcium conductances are thought to be fundamental to the initiation of firing and in the generation of pacemaker-like activity in certain neuronal types and in synchronisation of network activity (Llinas, 1988; Huguenard & McCormick, 1992).

In AD-SPN the T-type conductance was revealed following block of the transient outward rectification, suggesting the conductance is either apparent in specific circumstances or discretely distributed. Modulation of transient outward rectification by neurotransmitters could uncover the T-type calcium conductance. In relation to this, previous *in vitro* studies in SPN in adult cat have demonstrated noradrenaline-induced burst firing, mainly due to activation of an inward Ca^{2+} conductance (Yoshimura *et al.* 1987*b*). Noradrenaline also reduced the AHP and revealed an after-depolarisation potential (Yoshimura *et al.* 1986*c*) mediated by a Ca^{2+}-activated Na^+ conductance. After-depolarisation potentials that can underlie pacemaker-like activity have also been observed in the cat *in vivo* (Dembowsky *et al.* 1986) and in Cs^+-loaded SPN in adult cat *in vitro* (Yoshimura *et al.* 1987*c*). Taken together, these data demonstrate that SPN are potentially conditional pacemakers, i.e. under the influence of neurotransmitters, these cells can act as pacemakers and generate burst firing.

An alternative explanation is that there may be a differential localisation of channels over the SPN membrane. The impact of differential distributions of ion channels on the integrative capabilities of a neurone has been demonstrated previously in other central neurones (Hoffman *et al.* 1997; Johnston *et al.* 1999; Korngreen & Sakmann, 2000; Bekkers, 2000). For example, rhythmic activity mediated by T-type calcium conductances preferentially expressed in dendritic compartments can be modified by other intrinsic conductances (Destexhe *et al.* 1998).

Recognising that AD-SPN have the intrinsic capability for generating autorhythmicity and burst firing may have important functional implications. Previous studies have demonstrated that burst stimulation of the splanchnic nerve enhanced adrenaline and NA release but proportionately more NA than adrenaline; such stimuli also enhanced met-enkephalin release (Bloom *et al.* 1989). Further studies of AD-SPN are required to identify the molecular composition, localisation and role of these active conductances in integrating synaptic inputs, generating and shaping the sympathetic output to the adrenal gland.

Functional considerations

Results presented here suggest SPN innervating the adrenal medulla are, for the main part, a homogeneous population regarding the expression of their active conductances. Numerous physiological and anatomical studies suggest distinct neuronal pathways control adrenaline and NA release (e.g. see Folkow & von Euler, 1954; Gagner *et al.* 1985; Vollmer, 1996). The balance may be regulated at many levels of the neuraxis. At the level of the spinal cord, AD-SPN in cat have been shown to be subdivisible based on the presence of the calcium binding protein, calretinin (Edwards *et al.* 1996). In rat SPN innervating NA-containing chromaffin cells can be distinguished from those innervating adrenaline-containing chromaffin cells by their response to RVLM stimulation, chemoreceptor activation and reflex response to glucopenic stimuli (Morrison & Cao, 2000; Cao & Morrison, 2001). Noradrenaline chromaffin cell-innervating SPN discharge rate was strongly influenced by the baroreceptor reflex whilst both sets of SPN were inhibited by the Bezold–Jarish reflex (Cao & Morrison, 2000). These physiological responses suggest a functionally and anatomically distinct organisation of the autonomic pathways controlling adrenaline and NA release. A lack of obvious divergence in the expression patterns of active membrane conductances in our analysis and spontaneous firing patterns and axonal conduction velocity reported *in vivo* (Backman *et al.* 1990), suggest factors other than active conductances are key to the differential regulation of catecholamine secretion. In addition, we have identified a population of AD-SPN which are electrotonically coupled, and the subject of a separate paper, which may lend support to the argument for divergent pathways to the adrenal medulla that include a function-specific organisation of AD-SPN.

Conclusion

The present analysis reveals AD-SPN possess active conductances that impart the capability for dynamic and diverse central commands to the adrenal medulla. The largely homogeneous distribution of these active conductances across the AD-SPN population implies additional factors contribute to the differential regulation of adrenaline *versus* NA secretion. Such factors may include separate central circuits and differential synaptic influences to AD-SPN.

REFERENCES

An, W. F., Bowlby, M. R., Betty, M., Cao, J., Ling, H. P., Mendoza, G., Hinson, J. W., Mattsson, K. I., Strassle, B. W., Trimmer, J. S. & Rhodes, K. J. (2000). Modulation of A-type potassium channels by a family of calcium sensors. *Nature* **403**, 553–556.

Backman, S. B., Sequeira-Martinho, H. & Henry, J. L. (1990). Adrenal *versus* nonadrenal sympathetic preganglionic neurones in the lower thoracic intermediolateral nucleus of the cat: physiological properties. *Canadian Journal of Physiology and Pharmacology* **68**, 1447–1456.

Bahring, R., Dannenberg, J., Peters, H. C., Leicher, T., Pongs, O. & Isbrandt, D. (2001). Conserved Kv4 N-terminal domain critical for effects of Kv channel-interacting protein 2.2 on channel expression and gating. *Journal of Biological Chemistry* **276**, 23 888–23 894.

Bekkers, J. M. (2000). Distribution and activation of voltage-gated potassium channels in cell-attached and outside-out patches from large layer 5 cortical pyramidal neurones of the rat. *Journal of Physiology* **525**, 611–620.

Block, B. M. & Jones, S. W. (1997). Delayed rectifier current of bullfrog sympathetic neurones: ion–ion competition, asymmetrical block and effects of ions on gating. *Journal of Physiology* **499**, 403–416.

Bloom, S. R., Edwards, A. V. & Jones, C. T. (1988). The adrenal contribution to the neuroendocrine responses to splanchnic nerve stimulation in conscious calves. *Journal of Physiology* **397**, 513–526.

Bloom, S. R., Edwards, A. V. & Jones, C. T. (1989). Neuroendocrine responses to stimulation of the splanchnic nerves in bursts in conscious, adrenalectomized, weaned lambs. *Journal of Physiology* **417**, 79–89.

Cao, W. H. & Morrison, S. F. (2000). Responses of adrenal sympathetic preganglionic neurons to stimulation of cardiopulmonary receptors. *Brain Research* **887**, 46–52.

Cao, W. H. & Morrison, S. F. (2001). Differential chemoreceptor reflex responses of adrenal preganglionic neurons. *American Journal of Physiology – Regulatory, Integrative and Comparative Physiology* **281**, R1825–1832.

Casavant, R. H., Xu, Z. & Dryer, S. E. (2000). Fatty acid-activated K^+ channels in autonomic neurons: activation by an endogenous source of free fatty acids. *Journal of Neurochemistry* **74**, 1026–1033.

Cobbett, P., Legendre, P. & Mason, W. T. (1989). Characterization of three types of potassium current in cultured neurones of rat supraoptic nucleus area. *Journal of Physiology* **410**, 443–462.

Colbert, C. M. & Pan, E. (1999). Arachidonic acid reciprocally alters the availabilty of transient and sustained dendritic K^+ channels in hippocampal CA1 pyramidal neurons. *Journal of Neuroscience* **19**, 8163–8171.

Dembowsky, K., Czachurski, J. & Seller, H. (1986). Three types of sympathetic preganglionic neurones with different electrophysiological properties are identified by intracellular recordings in the cat. *Pflügers Archiv* **406**, 112–120.

Destexhe, A., Neubig, M., Ulrich, D. & Huguenard, J. (1998). Dendritic low-threshold calcium currents in thalamic relay cells. *Journal of Neuroscience* **18**, 3574–3588.

Edwards, A. V. & Jones, C. T. (1993). Autonomic control of adrenal function. *Journal of Anatomy* **183**, 291–307.

Edwards, S. L., Anderson, C. R., Southwell, B. R. & McAllen, R. M. (1996). Distinct preganglionic neurons innervate noradrenaline and adrenaline cells in the cat adrenal medulla. *Neuroscience* **70**, 825–832.

Folkow, B. & von Euler, U. S. (1954). Selective activation of noradrenaline and adrenaline producing cells in the cat's adrenal gland by hypothalamic stimulation. *Circulation Research* **11**, 191–195.

Gagner, J. P., Gauthier, S. & Sourkes, T. L. (1985). Descending spinal pathways mediating the responses of adrenal tyrosine hydroxylase and catecholamines to insulin and 2-deoxyglucose. *Brain Research* **325**, 187–197.

Griffin, J. D. & Boulant, J. A. (1995). Temperature effects on membrane potential and input resistance in rat hypothalamic neurones. *Journal of Physiology* **488**, 407–418.

Hoffman, D. A., Magee, J. C., Colbert, C. M. & Johnston, D. (1997). K^+ channel regulation of signal propagation in dendrites of hippocampal pyramidal neurons. *Nature* **387**, 869–875.

Holmqvist, M. H., Cao, J., Knoppers, M. H., Jurman, M. E., Distefano, P. S., Rhodes K. J., Xie, Y. & An, W. F. (2001). Kinetic modulation of Kv4-mediated A-current by arachidonic acid is dependent on potassium channel interacting proteins. *Journal of Neuroscience* **21**, 4154–4161.

Huguenard, J. R. (1996). Low-threshold calcium currents in central nervous system neurones. *Annual Review of Physiology* **58**, 329–348.

Huguenard, J. R. & McCormick, D. A. (1992). Simulation of currents involved in rhythmic oscillations in thalamic relay neurons. *Journal of Neurophysiology* **68**, 1373–1383.

Imai, S., Suzuki, T., Sato, K. & Tokimasa, T. (1999). Effects of quinine on three different types of potassium currents in bullfrog sympathetic neurons. *Neuroscience Letters* **275**, 121–124.

Inokuchi, H., Masuko, S., Chiba, T., Yoshimura, M., Polosa, C. & Nishi, S. (1993). Membrane properties and dendritic arborization of the intermediolateral nucleus neurons in the guinea-pig thoracic spinal cord *in vitro*. *Journal of the Autonomic Nervous System* **43**, 97–106.

Johnston, D., Hoffman, D. A., Colbert, C. M. & Magee, J. C. (1999). Regulation of back-propogating action potentials in hippocampal neurons. *Current Opinions in Neurobiology* **9**, 288–292.

Korngreen, A. & Sakmann, B. (2000). Voltage-gated K^+ channels in layer 5 neocortical pyramidal neurones from young rats: subtypes and gradients. *Journal of Physiology* **525**, 621–639.

Lee, J. H., Gomora, J. C., Cribbs, L. L. & Perez-Reyes, E. (1999*a*). Nickel block of three cloned T-type calcium channels: low concentrations selectively block alpha1H. *Biophysical Journal* **77**, 3034–3042.

Li, Z. & Ferguson, A. V. (1996). Electrophysiological properties of paraventricular magnocellular neurons in rat brain slices: modulation of IA by angiotensin II. *Neuroscience* **71**, 133–145.

Llinas, R. R. (1988). The intrinsic electrophysiological properties of mammalian central neurons: insights into central nervous system function. *Science* **242**, 1654–1664.

Logan, S. D., Pickering, A. E., Gibson, I. C., Nolan, M. F. & Spanswick, D. (1996). Electrotonic coupling between rat sympathetic preganglionic neurones *in vitro*. *Journal of Physiology* **95**, 491–502.

Marley, P. D. & Livett, B. G. (1987). Differences between the mechanisms of adrenaline and noradrenaline secretion from isolated, bovine, adrenal chromaffin cells. *Neuroscience Letters* **77**, 81–86.

Matsui, H. (1979). Adrenal medullary secretory response to stimulation of the medulla oblongata in the rat. *Neuroendocrinology* **29**, 385–390.

Matsui, H. (1987). Effect of subthalamic stimulation of adrenal epinephrine and norepinephrine secretion in the rat. *Brain Research* **417**, 158–160.

Meadows, H. J. & Randall, A. D. (2001). Functional characterisation of human TASK-3, an acid-sensitive two-pore domain potassium channel. *Neuropharmacology* **40**, 551–559.

Miyazaki, T., Dun, N. J., Kobayashi, H. & Tosaka, T. (1996). Voltage-dependent potassium currents of sympathetic preganglionic neurons in neonatal rat spinal cord thin slices. *Brain Research* **743**, 1–10.

Morrison, S. F. & Cao, W. H. (2000). Different adrenal sympathetic preganglionic neurons regulate epinephrine and norepinephrine secretion. *American Journal of Physiology – Regulatory, Integrative and Comparative Physiology* **279**, R1763–1775.

Nolan, M. F., Logan, S. D. & Spanswick, D. (1999). Electrophysiological properties of electrical synapses between rat sympathetic preganglionic neurones *in vitro*. *Journal of Physiology* **519**, 753–764.

Perez-Reyes, E. (1999). Three for T: molecular analysis of the low voltage-activated calcium channel family. *Cellular and Molecular Life Sciences* **56**, 660–669.

Pickering, A. E., Spanswick, D. & Logan, S. D. (1991). Whole-cell recordings from sympathetic preganglionic neurons in rat spinal cord slices. *Neuroscience Letters* **130**, 237–242.

Rajan, S., Wischmeyer, E., Xin Liu, G., Preisig-Muller, R., Daut, J., Karschin, A. & Derst, C. (2000). TASK-3, a novel tandem pore domain acid-sensitive K^+ channel. An extracellular histiding as pH sensor. *Journal of Biological Chemistry* **275**, 16650–16657.

Rathouz, M. & Trussell, L. (1998). Characterization of outward currents in neurons of the avian nucleus magnocellularis. *Journal of Neurophysiology* **80**, 2824–2835.

Robinson, R. L., Culberson, J. L. & Carmichael, S. W. (1983). Influence of hypothalamic stimulation on the secretion of adrenal medullary catecholamines. *Journal of the Autonomic Nervous System* **8**, 89–96.

Rogawski, M. (1985). The A-current. How ubiquitous a feature of excitable cells is it? *Trends in Neuroscience* **83**, 214–219.

Spanswick, D., Renaud, L. P. & Logan, S. D. (1998). Bilaterally evoked monosynaptic EPSPs, NMDA receptors and potentiation in rat sympathetic preganglionic neurones *in vitro*. *Journal of Physiology* **509**, 195–209.

Storm, J. F. (1990). Potassium currents in hippocampal pyramidal cells. *Progress in Brain Research* **83**, 161–187.

Strack, A. M., Sawyer, W. B., Marubio, L. M. & Loewy, A. D. (1988). Spinal origin of sympathetic preganglionic neurons in the rat. *Brain Research* **455**, 187–191.

Strack, A. M., Sawyer, W. B., Platt, K. B. & Loewy, A. D. (1989). CNS cell groups regulating the sympathetic outflow to adrenal gland as revealed by transneuronal cell body labelling with pseudorabies virus. *Brain Research* **491**, 274–296.

Tombaugh, G. C. & Somjen, G. G. (1996). Effects of extracellular pH on voltage-gated Na^+, K^+ and Ca^{2+} currents in isolated rat CA1 neurons. *Journal of Physiology* **493**, 719–732.

Trequattrini, C., Petris, A. & Franciolini, F. (1996). Characterization of a neuronal delayed rectifier K current permeant to Cs and blocked by verapamil. *Journal of Membrane Biology* **154**, 143–153.

Traynelis, S. F. (1998). pH modulation of ligand-gated ion channels. In *pH and Brain Function*, ed. Kaila, K. & Ransom, B. R. , pp. 417–446. Wiley-Liss, New York.

Vollmer, R. R. (1996). Selective neural regulation of epinephrine and norepinephrine cells in the adrenal medulla–cardiovascular implications. *Clinical Experimental Hypertension* **18**, 731–751.

Wigmore, M. A. & Lacey, M. G. (2000). A Kv3-like persistent, outwardly rectifying, Cs^+-permeable, K^+ current in rat subthalamic nucleus neurones. *Journal of Physiology* **527**, 493–506.

Yoshimura, M., Polosa, C. & Nishi, S. (1986*a*). After-hyperpolarization mechanisms in cat sympathetic preganglionic neuron *in vitro*. *Journal of Neurophysiology* **55**, 1234–1246.

Yoshimura, M., Polosa, C. & Nishi, S. (1986*b*). Electrophysiological properties of sympathetic preganglionic neurons in the cat spinal cord *in vitro*. *Pflügers Archiv* **406**, 91–98.

Yoshimura, M., Polosa, C. & Nishi, S. (1986*c*). Noradrenaline modifies sympathetic preganglionic neuron spike and after-potential. *Brain Research* **362**, 370–374.

Yoshimura, M., Polosa, C. & Nishi, S. (1987*a*). A transient outward rectification in the cat sympathetic preganglionic neuron. *Pflügers Archiv* **408**, 207–208.

Yoshimura, M., Polosa, C. & Nishi, S. (1987*b*). Noradrenaline induces rhythmic bursting in sympathetic preganglionic neurons. *Brain Research* **420**, 147–151.

Yoshimura, M., Polosa, C. & Nishi, S. (1987*c*). Afterdepolarization mechanism in the *in vitro*, cesium-loaded, sympathetic preganglionic neuron of the cat. *Journal of Neurophysiology* **57**, 1325–1337.

Acknowledgements

Operating support was provided by the Heart and Stroke Foundation of Canada (Grant no. T4466) and the Canadian Institutes for Health Research (Grant no. MOP-03822). J.W. is the recipient of a Canadian Commonwealth Graduate Scholarship and a Canadian Institutes for Health Research Studentship.